PCCP

On the concentration polarisation in molten Li salts and borate-based Li ionic liquids

Journal:	*Physical Chemistry Chemical Physics*
Manuscript ID	CP-ART-12-2022-005710.R1
Article Type:	Paper
Date Submitted by the Author:	13-Jan-2023
Complete List of Authors:	Shigenobu, Keisuke; Yokohama National University, Chemistry Philippi, Frederik; Yokohama National University, Department of Chemistry and Biotechnology Tsuzuki, Seiji; Yokohama National University, Institute of Advanced Sciences Kokubo, Hisashi; Yokohama Kokuritsu Daigaku Dokko, Kaoru; Yokohama National University, Department of Chemistry and Biotechnology Watanabe, Masayoshi; Yokohama National University, Chemistry andBiotechnology Ueno, Kazuhide; Yokohama National University, Department of Chemistry and Biotechnology

ARTICLE

On the concentration polarisation in molten Li salts and borate-based Li ionic liquids

Received 00th January 20xx,
Accepted 00th January 20xx

DOI: 10.1039/x0xx00000x

Keisuke Shigenobu,[a] Frederik Philippi,[a] Seiji Tsuzuki, [b] Hisashi Kokubo, [a] Kaoru Dokko, [a, b] Masayoshi Watanabe [b] and Kazuhide Ueno *[a, b]

Electrolytes that transport only Li ions play a crucial role in improving rapid charge and discharge properties in Li secondary batteries. The single Li-ion conduction can be achieved via liquid materials such as Li ionic liquids containing Li^+ as the only cations, because solvent-free fused Li salts do not polarise in electrochemical cells, owing to the absence of neutral solvents that allow polarisation in the salt concentration and the inevitably homogeneous density in the cells under anion-blocking conditions. However, we found that borate-based Li ionic liquids induce concentration polarisation in a Li/Li symmetric cell, which results in their transference (transport) numbers under anion-blocking condition ($t_{\mathrm{Li}}^{\mathrm{abc}}$) well below unity. The electrochemical polarisation of the borate-based Li ionic liquids was attributed to an equilibrium shift caused by exchangeable B–O coordination bonds in the anions to generate Li salts and borate-ester solvents at the electrode/electrolyte interface. By comparing borate-based Li ionic liquids containing different ligands, the B–O bond strength and extent of ligand exchange were directly linked to the $t_{\mathrm{Li}}^{\mathrm{abc}}$values. This study confirms that the presence of dynamic exchangeable bonds causes electrochemical polarisation and provides a reference for the rational molecular design of Li ionic liquids aimed at achieving single-ion conducting liquid electrolytes.

Introduction

Widespread use of electric vehicles and stationary energy storage is indispensable for renewable energy to become an efficient countermeasure against climate change. Lithium secondary batteries have been used in the applications as state-of-the-art energy storage. However, issues with power density, energy density, and fire safety remain unresolved. To meet the current demand for Li secondary batteries capable of rapid charge and discharge, the transport properties of liquid electrolytes, such as ionic conductivities and Li^+ transference (transport) numbers (t_{Li}), must be improved [1, 2]. Electrolytes with high t_{Li} also suppress Li dendrite formation, thereby boosting the development of high-energy-density Li metal batteries [3]. Previous studies have aimed at improving t_{Li} values, for instance, using metal/covalent organic frameworks (MOFs/COFs) [4-6], anion-receptor additives [7-10], polyanions [11-15], and highly concentrated electrolytes [16-18]. However, a partial Li salt concentration gradient is expected in electrochemical cells, unless single-ion conduction (t_{Li} ~ 1) has been achieved. An 18 % concentration difference between Li metal electrodes was indeed visualised via *in situ* magnetic resonance imaging (MRI) for a concentrated electrolyte comprising 3 mol dm^{-3} of $LiPF_6$ in ethyl methyl carbonate (EMC, $t_{\mathrm{Li}} \approx 0.4$) [19]. Such a high concentration polarisation significantly increases the overpotential, saturation/salt precipitation, and/or salt depletion at the electrode interface, which in turn causes battery degradation [20-22].

To completely suppress concentration polarisation under anion-blocking conditions, that is, to achieve single-ion conduction (t_{Li} ~ 1) in liquid electrolytes containing a salt dissolved in a molecular solvent, complex ionic motions must be considered. There has been a greater understanding of the ion transport by the fundamental and comprehensive works regarding the transference number including methodology [23-28], velocity of components [29-31] and frame of reference [27, 32-39], and mode of transport such as migration and diffusion (and in some cases convection) [27, 40-42]. Especially, mutual ion–ion and ion–solvent motions have been investigated in concentrated electrolytes based on various transport theories, using the velocity cross-correlation [43-47], Stefan–Maxwell diffusion [40, 48-50], and Onsager transport coefficients [28, 51, 52]. Although the concentrated electrolyte theory predicts the feasibility of t_{Li} being 1 in liquid electrolytes, highly elaborate modulations of the ion–ion and ion–solvent interactions are necessary for achieving a veritable single-ion conduction [28, 51, 53].

Ionic liquid-based electrolytes have been intensively studied as a non-flammable liquid electrolyte for enhancing battery safety [54-57]. However, binary mixtures of aprotic ionic liquids and Li salts dominate the previous reports, and studies on

[a] *Department of Chemistry and Life Science, Yokohama National University, 79-5 Tokiwadai, Hodogaya-ku, Yokohama 240-8501, Japan.*
[b] *Institute of Advanced Sciences, Yokohama National University, 79-5 Tokiwadai, Hodogaya-ku, Yokohama 240-8501, Japan.*

Electronic Supplementary Information (ESI) available: thermogravimetric data for $Li[B(OTFA)_4]$, NMR spectra of synthesised compounds, ^{11}B VT-NMR and FAB-MS spectra of $Li[B(mPEG3)_2(OHFIP)_2]$ and the B3LYP/6–311++G** level optimised structures of $Li[(OHFIP)_4]$ and $Li[(OTFA)_4]$ were summarised. See DOI: 10.1039/x0xx00000x

solvent-free molten Li salts or Li ionic liquids containing Li^+ as the only cations are largely limited because of their intrinsically high melting point. Considering the single-ion conduction, the solvent-free molten Li salts or Li ionic liquids can also achieve $t_{Li} \sim 1$ under anion-blocking conditions. A significant difference in the mass and momentum of Li^+ and bulky anions in the molten salt results in a highly preferential motion of Li^+ [28, 53, 58]. In addition, the density of the molten Li salts is invariable, and therefore, a concentration gradient of Li salt cannot be formed in electrochemical cells under anion-blocking conditions, even though the current passes through the electrode/electrolyte interface [59]. Indeed, a high t_{Li} value of 0.94 was achieved in an electrochemical cell using a molten Li salt, lithium (fluorosulfonyl) (trifluoromethanesulfonyl)amide (Li[FTA]) at 140 °C [60]. Counter anions have also been specially designed to lower the melting points of Li salts. Despite that, the high melting points of these salts restrict their use at room temperature [61-63].

Borate-based Li ionic liquids containing Li^+ as the only cations, as reported by us and Fujinami et al. [64-67], can remain in a liquid state at ambient temperatures (in a broad sense, below 100 °C) and can be used as liquid electrolytes owing to their good compatibility with Li metal electrodes and high oxidative stability (> 4 V) [68]. This unique room-temperature liquefaction was achieved by reducing the Lewis basicity of the borate-anion centre using electron-withdrawing ligands and enhancing the dissociability of Li^+ using oligoether (ethylene oxide (EO)) groups introduced into the anion.

Here, we evaluated the t_{Li} values of borate-based Li ionic liquids and compared them with those of other molten Li salts: Li[FTA] [60] and lithium 2,5,8,11-tetraoxatridecan-13-oate (Li[TOTO]) [69]. An unfavourable concentration polarisation was observed in an electrochemical cell using the borate-based Li ionic liquids. We investigated the possible factors causing unfavourable electrochemical polarisation and proposed a method to mitigate them in borate-based Li ionic liquids.

Experimental

Syntheses

Borate-based Li ionic liquids, lithium bis(2-(2-(2-methoxyethoxy)ethoxy)ethoxy)-bis(hexafluoroisopropyloxy)borate ($Li[B(mPEG3)_2(OHFIP)_2]$) and lithium bis(2-(2-(2-methoxyethoxy)ethoxy)ethoxy)-bis(2,2,2-trifluoroacetoxy)borate ($Li[B(mPEG3)_2(OTFA)_2]$), and Li salts, lithium tetrakis(2-(2-(2-methoxyethoxy)ethoxy)ethoxy)borate ($Li[B(mPEG3)_4]$) and lithium tetrakis(2,2,2-trifluoroacetoxy)borate ($Li[B(OTFA)_4]$), were synthesised according to previously reported procedures [64, 65]. Another Li ionic liquid, Li[TOTO], was synthesised using the method reported by Zech et al., with a slight modification; zeolite molecular sieves (Tosoh, Zeolum NSA-700) were used for the purification process, instead of ultrahigh vacuum [69]. A borate-ester solvent, $B(mPEG3)_3$, was synthesised according to the method reported by Karatas et al. [70]. Figure **1** shows the chemical structures of the obtained compounds. The compounds were transferred to an inert Ar-filled glove box and characterised using ^1H and ^{11}B NMR spectroscopy. The NMR spectra of the synthesised compounds (except the borate-based Li ionic liquids) have been summarised in the supplementary information (**Figures S2–S6,** see Supplementary Information).

Measurements

^1H, ^{11}B, and ^{13}C NMR (only for Li[TOTO]), (JEOL, ECX400) were used for the characterisation of the synthesised compounds. A coaxial NMR tube system was used for the ^{11}B NMR measurements. The reference standards used were tetramethylsilane (TMS) for ^1H and ^{13}C NMR and a boron trifluoride-diethyl ether complex for ^{11}B NMR (δ = 0 ppm), and the synthesised compounds and the references were diluted using deuterated chloroform ($CDCl_3$). For the coaxial NMR tube system, the samples were inserted into the inner tube and the reference solutions were placed in the outer tube. Variable temperature (VT) ^{11}B NMR was also performed using the same coaxial-tube system, without diluting the borate-based Li ionic

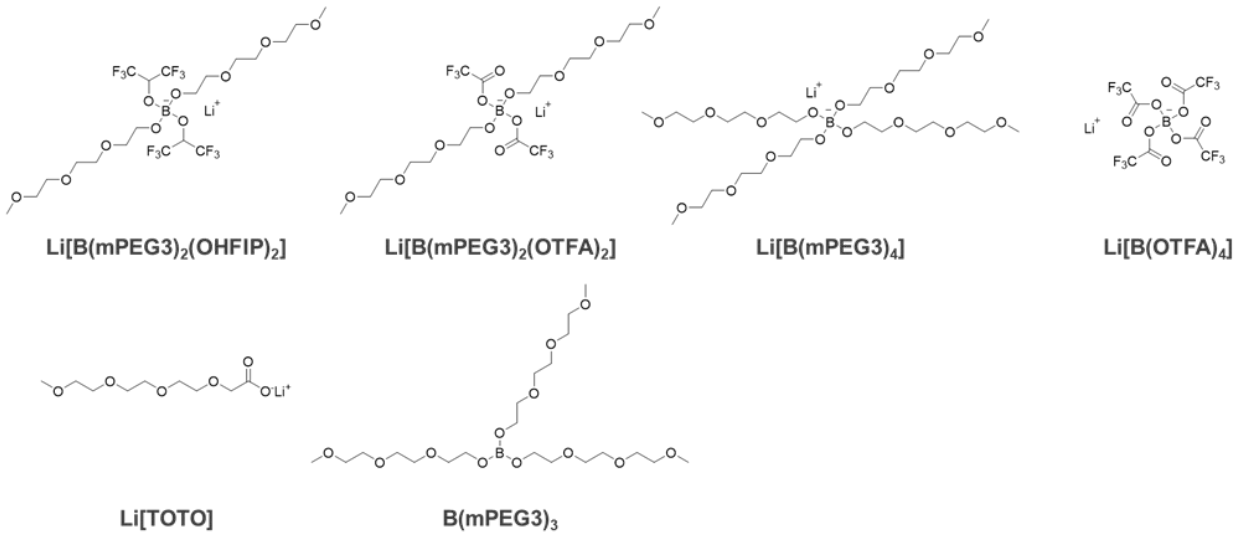

Figure 1 The chemical structures of the synthesised compounds.

liquids. A 1:10 molar-ratio mixture of $LiBF_4$ and deuterated dimethyl sulfoxide (DMSO-d_6) was used as the reference standard (δ = −0.82 ppm), because the reference solution maintained in a liquid state over the measurement-temperature range.

The Li^+ transference number under anion-blocking conditions (t_{Li}^{abc}) was determined by combining potentiostatic polarisation and electrochemical impedance spectroscopy using Li symmetric cells [71, 72].

Fast atom bombardment mass spectroscopy (FAB-MS) (JEOL, JMS-MS600) was performed in the positive-ion mode, using argon as the bombarding gas. The samples were collected without dilution, under air, owing to the probe setup.

Computational method

DFT calculations were performed using the Gaussian 16 program [73]. The geometries of the Li ionic liquids, borate esters, and Li salts were made through GaussView 6 and optimised at the B3LYP/6-311++G** level [74-77]. Before preparing the Li salts, each component (Li cation and anions) was made and optimised. For the borate esters, several possible structures were made considering the conformation. After the optimisation, for the Li salts, the possible geometries such as monodentate or bidentate were considered. The number of possible initial structures for $Li[B(OHFIP)_4]$ and $Li[B(OTFA)_4]$ was 3 and 5, respectively. The interaction energies between Li^+ and anions for the possible geometries were first calculated, and then the geometries with the lowest energy were employed for the main calculation (total energy). The basis set superposition error (BSSE) [78] was corrected by counterpoise method [79] for the interaction energy calculation. The energies for these components (E_{LiIL}, E_{sol}, and E_{salt}, respectively) were calculated at the same level as the optimisation. The energy difference (heat of reaction, ΔE) was calculated using **Eq. 2** at the B3LYP/6-311++G** level.

Results and discussion

Transport properties of Li ionic liquids

Various methods have been proposed to estimate Li^+ transference numbers. Here, we used an electrochemical method based on potentiostatic polarisation combined with electrochemical impedance spectroscopy [71, 72]. The transference number (t_{Li}^{abc}) obtained using this method under the anion-blocking condition, referred as "current fraction" [80], can be defined as follows:

$$t_{Li}^{abc} = \frac{I_{SS}(V_{DC} - I_{Ohm}R_{i,0})}{I_{Ohm}(V_{DC} - I_{SS}R_{i,SS})} \#(\text{Eq. } 1),$$

where V_{DC} is a constant applied voltage, I_{Ohm} and I_{SS} are the initial and steady-state currents, respectively, and $R_{i,0}$ and $R_{i,SS}$ are the initial and steady-state interfacial resistances, respectively. I_{Ohm} was calculated using Ohm's law, $I_{Ohm} = V_{DC}/(R_{bulk} + R_{i,0})$, owing to the inaccuracy of "measured" initial current data point (I_0), which strongly depends on the sampling time [80]. In this method, t_{Li}^{abc} is obtained in the laboratory frame of reference.

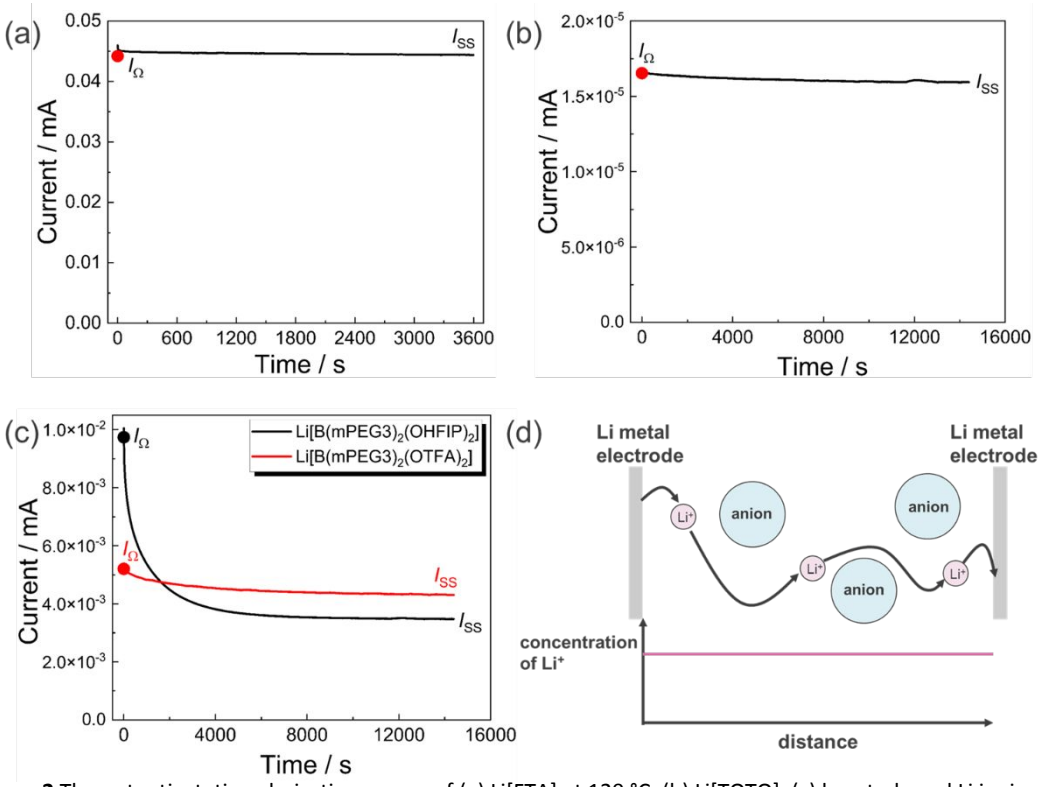

Figure 2 The potentiostatic polarisation curves of (a) Li[FTA] at 120 °C, (b) Li[TOTO], (c) borate-based Li ionic liquids at 30 °C, and (d) schematic image of no concentration polarisation ($t_{Li}^{abc} \sim 1$) and its concentration profile.

Figure 2 (a) shows the potentiostatic polarisation curve of the inorganic molten Li salt, lithium(fluorosulfonyl)(trifluoromethanesulfonyl)amide (Li[FTA]), at 120 °C. The current decay with time was negligible, suggesting that no concentration gradient was formed in the Li/Li symmetric electrochemical cell. The $t_{\mathrm{Li}}^{\mathrm{abc}}$ of the molten Li[FTA] salt was calculated to be 0.99. Thus, we could reproduce the results reported for Li[FTA] by Kubota *et al* [60, 81]. We also measured the $t_{\mathrm{Li}}^{\mathrm{abc}}$ of a room-temperature Li ionic liquid, Li[TOTO], which contained an mPEG3 chain covalently bound to a carboxylate anion. We could not determine the accurate $t_{\mathrm{Li}}^{\mathrm{abc}}$ value of Li[TOTO] because of the severe overlap between R_{bulk} and $R_{\mathrm{i},0}$ in the impedance spectra. Nevertheless, I_{SS} was approximately equal to I_{Ohm}, similar to Li[FTA]; therefore, the concentration polarisation is expected to be negligible in the corresponding Li symmetric cell (**Figure 2 (b)**), and $t_{\mathrm{Li}}^{\mathrm{abc}}$ value of Li[TOTO] was assumed to be ~1. For molten Li salts, such as Li[FTA] and Li[TOTO], a spatial distribution of density is impossible in the absence of solvents during electrochemical polarisation, even if they are dissociated into Li^+ and counter anions, that is, the density must be homogeneous in the cells. Furthermore, the total momentum of ions in the electrochemical cell is conserved by ions when they move in the same manner as the common molten salts and ionic liquids [82-84]. Consequently, only Li^+ is mobile enough to maintain the density of Li ionic liquids and conserve the total momentum of ions (i.e., Li^+ can only conserve its momentum) in anion-blocking cells [85] (**Figure 2 (d)**). Thus, the estimated transference number ($t_{\mathrm{Li}}^{\mathrm{abc}}$) becomes 1. Interestingly, $t_{\mathrm{Li}}^{\mathrm{abc}}$ of the molten Li salts is in accordance with the cationic transference number of pure fused salts in the anion-fixed frame of reference as predicted in the Sinistri's work [32]. This would be related to the fact that the anion flux is zero under anion-blocking conditions. In contrast to the polarisation curves for molten Li[FTA] and Li[TOTO], current relaxation was observed in both $Li[B(mPEG3)_2(OHFIP)_2]$ and $Li[B(mPEG3)_2(OTFA)_2]$, suggesting that the cells were polarised under an electric field (**Figure 2 (c)**). The estimated $t_{\mathrm{Li}}^{\mathrm{abc}}$ values were lower than unity, but they showed a significant structure-dependence: a higher value of $t_{\mathrm{Li}}^{\mathrm{abc}}$ (0.77) was obtained for $Li[B(mPEG3)_2(OTFA)_2]$ compared with that of $Li[B(mPEG3)_2(OHFIP)_2]$ (0.25) at 30 °C.

Mechanism of the electrochemical polarisation in borate-based Li ionic liquids

Here, we discuss the reasons for the electrochemical polarisation in borate-based Li ionic liquids and the difference between the polarisation behaviours of $Li[B(mPEG3)_2(OHFIP)_2]$ and $Li[B(mPEG3)_2(OTFA)_2]$.

The first reason for polarisation would be the reversible ligand exchange of B–O bonds in the borate-based Li ionic liquids, which is not common in molten salts and ionic liquids. **Figures 3 (a) and (b)** show the ^{11}B NMR spectra of $Li[B(mPEG3)_2(OHFIP)_2]$ and $Li[B(mPEG3)_2(OTFA)_2]$, respectively. The broad background signals in the measurement range of 60 to −60 ppm can be attributed to the borosilicate-glass NMR tubes. These Li ionic liquids were synthesised via a two-step substitution reaction of $LiBH_4$ (see SI), and the signal

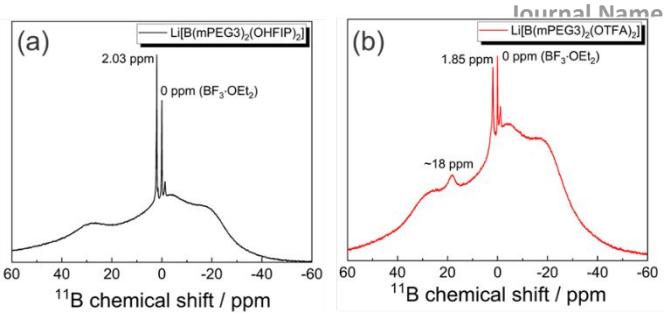

Figure 3 ^{11}B NMR spectra of (a) $Li[B(mPEG3)_2(OHFIP)_2]$ and (b) $Li[B(mPEG3)_2(OTFA)_2]$, from 60 to −60 ppm. The spectra were recorded at room temperature.

corresponding to the BH_4 anions (δ = −38.2 ppm, quintet) [86] was not confirmed in either Li ionic liquid, indicating a substitution reactions proceeded successfully. In addition, a sharp signal at approximately 2 ppm (δ = 2.03 and 1.85 ppm for $Li[B(mPEG3)_2(OHFIP)_2]$ and $Li[B(mPEG3)_2(OTFA)_2]$, respectively) was assigned to the $B(OR)_4$ (R: mPEG3, HFIP, and TFA) anion mixtures, along with the ligand exchange based on the chemical shifts of $Li[B(mPEG1)_4]$ (δ = 2.64 ppm) [87], $Li[B(mPEG3)_4]$ (δ = 2.63 ppm, **Figure S3 (b)**), $Li[B(OTFA)_4]$ (δ = 1.27 ppm, **Figure S4**), and $Li[B(OHFIP)_4]$•3DME (δ = 1.54 ppm, in DMSO-D_6) [63]. Therefore, $Li[B(mPEG3)_2(OTFA)_2]$ and $Li[B(mPEG3)_2(OHFIP)_2]$ were considered the nominal compositions; however, they were actually composed of a mixture of $Li[B(mPEG3)_x(OTFA)_{4-x}]$ and $Li[B(mPEG3)_x(OHFIP)_{4-x}]$ (x = 0–4).

The borate ester (B–O) bond is an exchangeable covalent bond, and its bond stability is controlled by the temperature and Lewis basicity of the ligands [88, 89]. To verify the ligand exchange of the B–O bonds, VT NMR spectroscopy was conducted. **Figure 4** shows the temperature-dependent ^{11}B spectra of $Li[B(mPEG3)_2(OTFA)_2]$. Two sharp signals were observed between 0–3 ppm at 5 °C, and the signal with a higher chemical shift was assigned to the mPEG3-rich mixture of $[B(mPEG3)_x(OTFA)_{4-x}]^-$ (denoted as mPEG3-rich anion) and the one with a lower chemical shift to the OTFA-rich $[B(mPEG3)_x(OTFA)_{4-x}]^-$ (denoted as OTFA-rich anion), according to the ^{11}B chemical shifts of their Li salts: $Li[B(mPEG3)_4]$ (δ = 2.63 ppm, **Figure S3 (b)**) and $Li[B(OTFA)_4]$ (δ = 1.27 ppm, **Figure S4**). The two signals gradually coalesced with increasing temperature and became a single broad signal at temperatures higher than 40 °C, suggesting that the ligand exchange of B–O bonds occurred between the borate-ester anions at a timescale lower than the NMR timescale. In contrast, multiple ^{11}B chemical shifts corresponding to mPEG3-rich $[B(mPEG3)_x(OHFIP)_{4-x}]^-$ were observed at 2.14, 2.56, and 2.75 ppm, in addition to the shifts of OHFIP-rich $[B(mPEG3)_x(OHFIP)_{4-x}]^-$ (δ = 1.72 ppm) at 15 °C for $Li[(mPEG3)_2(OHFIP)_2]$ (**Figure S7**). The chemical shifts of the mPEG3-rich and OTFA-rich $[B(mPEG3)_x(OTFA)_{4-x}]^-$ anions gradually coalesced with increasing temperature, and a sharp signal was observed at 80 °C (**Figure 4**). In contrast to $Li[B(mPEG3)_2(OTFA)_2]$, the coalescence of the two signals was not observed for $Li[(mPEG3)_2(OHFIP)_2]$ (**Figure S7**). This suggests that the rate of ligand exchange of the B–O bonds

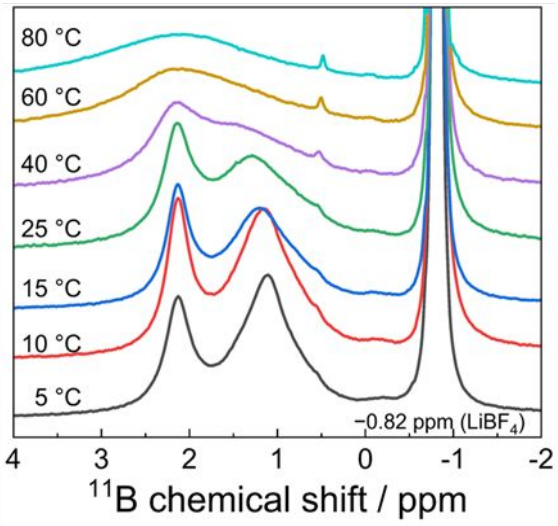

Figure 4 VT NMR spectra corresponding to ^{11}B of Li[B(mPEG3)$_2$(OTFA)$_2$].

between [B(mPEG3)$_4$]$^-$ and [B(OHFIP)$_4$]$^-$ was lower than the NMR timescale.

Considering the previously mentioned ligand exchange behaviour of the B–O bonds in the borate-ester anions, another competitive ligand exchange between the strong Lewis acid, Li$^+$, and the borate-ester solvents (B(OR)$_3$) may be possible in the Li ionic liquid via the dissociation of the alkoxide or trifluoroacetate ligands from the borate centre. Thus, the polarisation was mainly attributed to an equilibrium shift from the "solvent-free" borate-based Li ionic liquids to a electrolyte solution consisting of trivalent borate-ester solvents (B(OR)$_3$) and Li salts (see **Eq. 2**), owing to the ligand exchange of B–O bonds. As shown in **Figure 3 (b)**, a broad signal at approximately 18 ppm was confirmed for Li[B(mPEG3)$_2$(OTFA)$_2$] and was assigned to trivalent borate-ester solvents according to their signals: B(mPEG3)$_3$ (δ = 18.2 ppm, **Figure S5 (b)**), B(OCH$_3$)$_3$, and B(OC$_2$H$_5$)$_3$ (δ = 18.1 ppm) [86]. During the substitution reaction of LiBH$_4$, trivalent borate esters such as B(mPEG3)$_3$ would not be produced during the Li ionic liquid synthesis process. However, once the Li ionic liquid is formed, the following equilibrium can be assumed based on B–O bond exchange:

$$\mathrm{Li[B(mPEG3)_2(OTFA)_2]} \rightleftarrows \mathrm{LiOTFA} + \mathrm{B(mPEG3)_2(OTFA)} \quad \#(\mathrm{Eq.\ 2})$$

Li ionic liquids can generate Li salts and trivalent borate-ester solvents. The ^{11}B NMR results clearly indicated that the borate-based Li ionic liquid existed in equilibrium, and trivalent borate-ester solvents were generated at ambient temperature. For Li[B(mPEG3)$_2$(OHFIP)$_2$], the broad signal at 18 ppm (assigned to the trivalent borate-ester solvents) was not discernible, because it overlapped with the larger background spectra in **Figure 3 (a)**. However, Li[B(mPEG3)$_2$(OHFIP)$_2$] potentially generated solvent species in form of borate esters.

The FAB-MS spectra of Li[B(mPEG3)$_2$(OTFA)$_2$] (**Figure 5)** were obtained to validate the presumed mixture composition. The ionic liquid decomposed into positively ionised species and was detected in a gaseous state during the measurement. The base peak (*m/z* 171) was attributed to Li$^+$-coordinated mPEG3–OH, which was produced via fragmentation during the measurement. Here, *m/z* 577 was assigned to Li$^+$-coordinated Li[B(mPEG3)$_2$(OTFA)$_2$] (i.e., [Li$_2$[B(mPEG3)$_2$(OTFA)$_2$]]$^+$), indicating the synthesis of Li[B(mPEG3)$_2$(OTFA)$_2$] was successful. Moreover, the Li salt, LiOTFA (*m/z* 127: Li$^+$-coordinated one ([Li$_2$OTFA]$^+$)) and borate-ester solvents such as B(mPEG3)$_3$ (*m/z* 507: Li$^+$-coordinated), B(OLi)(mPEG3)$_2$ (*m/z* 367: Li$^+$-coordinated), and B(OLi)(OTFA)$_2$ (*m/z* 267: Li$^+$-coordinated) were detected in the Li ionic liquid. Similar to Li[B(mPEG3)$_2$(OTFA)$_2$], borate-ester solvents, B(mPEG3)$_3$ (*m/z* 507: Li$^+$-coordinated) and B(OLi)(mPEG3)$_2$ (*m/z* 367: Li$^+$-coordinated), were also observed in addition to Li$^+$-coordinated Li ionic liquids (*m/z* 677) in Li[B(mPEG3)$_2$(OHFIP)$_2$] (**Figure S8**). Therefore, the FAB-MS spectra suggest that borate-ester solvents can be generated via ligand exchange of B–O bonds, and the electrolyte solution species can coexist with borate-based Li ionic liquids.

According to the previously mentioned results, Li ionic liquids can be partially converted to Li salts and borate-ester solvents and behave as "liquid-electrolyte solutions", consequently forming a Li salt concentration gradient in electrochemical cells. Like concentrated electrolytes, solvents can contribute to momentum conservation by solvating and exchanging the ligand solvents and causing salt diffusion [51, 84]. Consequently, polarisation is possible in the electrochemical cells, and $t_{\mathrm{Li}}^{\mathrm{abc}}$ cannot be unity as long as borate-ester solvents exist therein.

If Li ionic liquids retain the "pure" ionic liquid character without equilibrium, like the molten Li salts, they would not be polarised under an electric field and the transference number under anion blocking conditions should be unity, *cf.* the polarisation curve of Li[FTA] and Li[TOTO]. Accordingly, the strength of the B–O exchangeable sites, which facilitate equilibrium (Eq. 2), determines the concentration polarisation in the electrochemical cells.

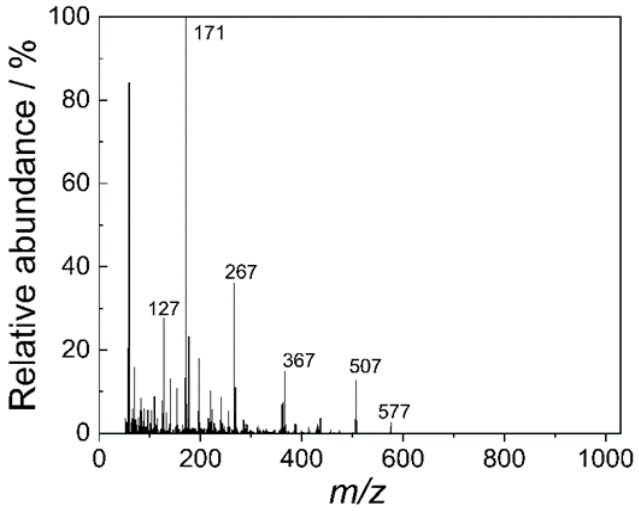

Figure 5 FAB-MS spectrum of ^{11}B of Li[B(mPEG3)$_2$(OTFA)$_2$].

Herein, we discuss the difference in the $t_{\mathrm{Li}}^{\mathrm{abc}}$ of Li[B(mPEG3)$_2$(OHFIP)$_2$] and Li[B(mPEG3)$_2$(OTFA)$_2$], which arises from difference in the extent to which electrolyte solutions are generated in these Li ionic liquids. Compared with Li[B(mPEG3)$_2$(OTFA)$_2$], a larger amount of electrolyte solution

was formed in Li[B(mPEG3)$_2$(OHFIP)$_2$], owing to the more prominent right-shift of the equilibrium in Eq. 2, which resulted in a lower value of $t_{\mathrm{Li}}^{\mathrm{abc}}$ for Li[B(mPEG3)$_2$(OHFIP)$_2$]. We could not estimate the equilibrium constant directly from NMR measurements, because of the timescale and multiple conceivable species. Therefore, we estimated the extent to which the equilibrium had shifted to the right by comparing the energy difference (heat of reaction: ΔE) between the Li ionic liquids and electrolyte solutions (borate esters and Li salts), assuming the gaseous state, based on Eq. 2. We used Li[(OHFIP)$_4$] and Li[(OTFA)$_4$] as models of Li ionic liquids for simplicity of the DFT calculations and optimised structures (**Figure S9)**. **Table 1** summarises the energy difference between Li ionic liquids, and solvents and Li salts ($\Delta E = (E_{\mathrm{sol}} + E_{\mathrm{salt}}) - E_{\mathrm{LiIL}}$) and calculated total energies of the Li ionic liquid models, corresponding borate esters, and Li salts (E_{LiIL}, E_{sol}, and E_{salt}) were summarised in **Table S1**.

The calculated ΔE values for the equilibrium for Li[(OHFIP)$_4$] and Li[(OTFA)$_4$] were 151.49 and 202.69 kJ mol^{-1}, respectively. Therefore, the Li ionic liquids with the OHFIP group preferentially generated borate esters and Li salts, which accelerated the concentration polarisation in the cells more than Li[(OTFA)$_4$]. Indeed, $t_{\mathrm{Li}}^{\mathrm{abc}}$ for Li[B(mPEG3)$_2$(OHFIP)$_2$] was lower than that for Li[B(mPEG3)$_2$(OHFIP)$_2$], as mentioned in Section 3.2. The positive ΔE value for the equilibrium shown in Eq. 2 implies that the reverse reaction (left-shift) was predominant in both systems. However, in these calculations, no interaction between the generated borate esters and Li salts (i.e., stabilisation via solvation) was assumed in the gaseous state. Although the entropic contribution is not considered in the calculation, the forward shift in Eq. 2 is entropically favourable. Thus, electrolyte solution generation reactions (the right-shift of Eq. 2) were possible, considering entropic and solvation contributions, as evidenced by the NMR and FAB-MS spectra. Thus, the difference between the functional groups (e.g., OHFIP, OTFA, and mPEG3) in the borate-based Li ionic liquids affected the B–O exchange properties, as suggested by the difference in ΔE, which would in turn affect the $t_{\mathrm{Li}}^{\mathrm{abc}}$ value for the Li ionic liquids.

Although the borate-based Li ionic liquids showed concentration polarisation in the electrochemical cells, they were beneficial for transport properties, as shown in **Table 2,** in addition to room-temperature liquefaction. Indeed, borate-based Li ionic liquids were significantly less viscous than others (e.g., 590 mPa s at 30 °C for Li[B(mPEG3)$_2$(OHFIP)$_2$] vs. 17000 mPa s at 110 °C for Li[FTA] [60, 64] and 760000 mPa s at 30 °C for Na[TOTO] [69]).

Table 1 The energy difference (ΔE) between Li ionic liquids, and borate esters and Li salts [a].

	ΔE/kJ mol^{-1}
Li[B(OHFIP)$_4$]	151.49
Li[B(OTFA)$_4$]	202.69

a: Energy in kJ mol^{-1}. $\Delta E = (E_{\mathrm{sol}} + E_{\mathrm{salt}}) - (E_{\mathrm{LiIL}})$

Table 2 Conductivities and Li$^+$ transference numbers ($t_{\mathrm{Li}}^{\mathrm{abc}}$) of Li ionic liquids at 30 °C.

	Conductivity /S cm^{-1}	$t_{\mathrm{Li}}^{\mathrm{abc}}$
Li[B(mPEG3)$_2$(OHFIP)$_2$]	1.3×10^{-5} [a]	0.25
Li[B(mPEG3)$_2$(OTFA)$_2$]	2.7×10^{-5} [b]	0.77
Li[TOTO]	4.1×10^{-8}	~1

a: ref. 64 and b: ref. 65.

Thus, borate-based Li ionic liquids provided a higher room-temperature conductivity (e.g., 1.3×10^{-5} S cm^{-1} at 30 °C for Li[B(mPEG3)$_2$(OHFIP)$_2$]) [64] than Li ionic liquids (4.1×10^{-8} S cm^{-1} at 30 °C for Li[TOTO]). A comparative analysis of the $t_{\mathrm{Li}}^{\mathrm{abc}}$ values of Li[B(mPEG3)$_2$(OTFA)$_2$] and Li[B(mPEG3)$_2$(OHFIP)$_2$] suggested that a weaker Lewis-basicity ligand of the borate-ester anions mitigated the unfavourable formation of the electrolyte solution species (borate esters and Li salts as a by-product) and consequently an ionic-liquid-rich composition at equilibrium (Eq. 2), resulting in a higher $t_{\mathrm{Li}}^{\mathrm{abc}}$ value. Further rational design of the borate-ester anions may achieve higher $t_{\mathrm{Li}}^{\mathrm{abc}}$ and ionic conductivities of the Li ionic liquids.

Conclusions

Borate-based Li ionic liquids were polarised in electrochemical cells, in contrast to the molten Li[FTA] salt and "mPEG3-chain covalently bound" Li[TOTO] ionic liquids. This polarisation property was ascribed to the electrolyte-solution-generating equilibrium (Eq. 2), owing to the exchangeable B–O bonds in the Li ionic liquids. The energy difference (heat of reaction, ΔE) at equilibrium (Eq. 2) played an important role in maintaining a "pure" Li ionic liquid character; the significant electrochemical polarisation of Li[B(mPEG3)$_2$(OHFIP)$_2$] was ascribed to a lower energy barrier in the electrolyte-solution-generation reaction (Eq. 2) corresponding to Li[(OHFIP)$_4$] and Li[(OTFA)$_4$], using DFT calculations. Overall, this study emphasises that the presence of dynamic exchangeable bonds in Li ionic liquids causes electrochemical polarisation under anion-blocking conditions. For future work, we investigate borate-ester anions with weakly Lewis basic ligands to enhance $t_{\mathrm{Li}}^{\mathrm{abc}}$ and ionic conductivities of Li ionic liquids.

Author Contributions

Keisuke Shigenobu: conceptualisation, investigation (syntheses, characterisations and electrochemical measurements), methodology, project administration, visualisation and writing (original draft and revision). Frederik Philippi: writing (review and revision). Seiji Tsuzuki: investigation (DFT calculation) and resources (computational resources). Hisashi Kokubo: funding acquisition,

resources (facility of syntheses) and writing (review). Kaoru Dokko: funding acquisition and resources (electrochemical equipment) and writing (review). Masayoshi Watanabe: funding acquisition and writing (review). Kazuhide Ueno: conceptualisation, funding acquisition, resources (electrochemical equipment), supervision and writing (original draft and revision).

Conflicts of interest

There are no conflicts to declare.

Acknowledgements

We thank Mr. Shinji Ishihara (Instrumental Analysis Centre, Yokohama National University) for technical assistance with the FAB-MS. This study was supported in part by the JSPS KAKENHI (Grant Nos. 22J11851 to K. S., 22F22775 to F. P., 20H02837 and 22K19082 to K. U., 20K05628 to H. K., and 19H05812 and 22H00340 to K. D.) from the Japan Society for the Promotion of Science (JSPS), and by JST ALCA-SPRING Grant Number JPMJAL1301, Japan. This study is also based on results obtained from a project, JPNP20004, subsidized by the New Energy and Industrial Technology Development Organization (NEDO).

References

1. M. Doyle, T. F. Fuller and J. Newman, *Electrochimica Acta*, 1994, **39**, 2073-2081.
2. K. M. Diederichsen, E. J. McShane and B. D. McCloskey, *ACS Energy Letters*, 2017, **2**, 2563-2575.
3. P. Barai, K. Higa and V. Srinivasan, *Journal of The Electrochemical Society*, 2018, **165**, A2654-A2666.
4. J. H. Park, K. Suh, M. R. Rohman, W. Hwang, M. Yoon and K. Kim, *Chemical Communications*, 2015, **51**, 9313-9316.
5. M. Farina, B. B. Duff, C. Tealdi, A. Pugliese, F. Blanc and E. Quartarone, *ACS Applied Materials & Interfaces*, 2021, **13**, 53986-53995.
6. X. Wu, K. Chen, Z. Yao, J. Hu, M. Huang, J. Meng, S. Ma, T. Wu, Y. Cui and C. Li, *Journal of Power Sources*, 2021, **501**, 229946.
7. M. M. Anne and F. Tatsuo, *Chemistry Letters*, 1997, **26**, 915-916.
8. M. A. Mehta, T. Fujinami and T. Inoue, *Journal of Power Sources*, 1999, **81-82**, 724-728.
9. Y. M. Lee, J. E. Seo, N.-S. Choi and J.-K. Park, *Electrochimica Acta*, 2005, **50**, 2843-2848.
10. M. Kalita, M. Bukat, M. Ciosek, M. Siekierski, S. H. Chung, T. Rodríguez, S. G. Greenbaum, R. Kovarsky, D. Golodnitsky, E. Peled, D. Zane, B. Scrosati and W. Wieczorek, *Electrochimica Acta*, 2005, **50**, 3942-3948.
11. R. Bouchet, S. Maria, R. Meziane, A. Aboulaich, L. Lienafa, J.-P. Bonnet, T. N. T. Phan, D. Bertin, D. Gigmes, D. Devaux, R. Denoyel and M. Armand, *Nature Materials*, 2013, **12**, 452-457.
12. L. Porcarelli, A. S. Shaplov, F. Bella, J. R. Nair, D. Mecerreyes and C. Gerbaldi, *ACS Energy Letters*, 2016, **1**, 678-682.
13. H. G. Buss, S. Y. Chan, N. A. Lynd and B. D. McCloskey, *ACS Energy Letters*, 2017, **2**, 481-487.
14. H. Zhang, C. Li, M. Piszcz, E. Coya, T. Rojo, L. M. Rodriguez-Martinez, M. Armand and Z. Zhou, *Chemical Society Reviews*, 2017, **46**, 797-815.
15. S. Kondou, Y. Sakashita, X. Yang, K. Hashimoto, K. Dokko, M. Watanabe and K. Ueno, *ACS Applied Materials & Interfaces*, 2022, **14**, 18324-18334.
16. L. Suo, Y.-S. Hu, H. Li, M. Armand and L. Chen, *Nature Communications*, 2013, **4**, 1481.
17. K. Dokko, D. Watanabe, Y. Ugata, M. L. Thomas, S. Tsuzuki, W. Shinoda, K. Hashimoto, K. Ueno, Y. Umebayashi and M. Watanabe, *The Journal of Physical Chemistry B*, 2018, **122**, 10736-10745.
18. G. Åvall, J. Wallenstein, G. Cheng, K. L. Gering, P. Johansson and D. P. Abraham, *Journal of The Electrochemical Society*, 2021, **168**, 050521.
19. A. A. Wang, A. B. Gunnarsdóttir, J. Fawdon, M. Pasta, C. P. Grey and C. W. Monroe, *ACS Energy Letters*, 2021, **6**, 3086-3095.
20. V. Srinivasan and J. Newman, *Journal of The Electrochemical Society*, 2004, **151**, A1517.
21. L. S. Kremer, T. Danner, S. Hein, A. Hoffmann, B. Prifling, V. Schmidt, A. Latz and M. Wohlfahrt-Mehrens, *Batteries & Supercaps*, 2020, **3**, 1172-1182.
22. Z. Du, D. L. Wood, C. Daniel, S. Kalnaus and J. Li, *Journal of Applied Electrochemistry*, 2017, **47**, 405-415.
23. M. Gouverneur, J. Kopp, L. van Wüllen and M. Schönhoff, *Physical Chemistry Chemical Physics*, 2015, **17**, 30680-30686.
24. A. Ehrl, J. Landesfeind, W. A. Wall and H. A. Gasteiger, *Journal of The Electrochemical Society*, 2017, **164**, A2716.
25. A. Ehrl, J. Landesfeind, W. A. Wall and H. A. Gasteiger, *Journal of The Electrochemical Society*, 2017, **164**, A826.
26. H. J. Walls and T. A. Zawodzinski, *Electrochemical and Solid-State Letters*, 2000, **3**, 321.
27. T. Hou and C. W. Monroe, *Electrochimica Acta*, 2020, **332**, 135085.
28. N. M. Vargas-Barbosa and B. Roling, *ChemElectroChem*, 2020, **7**, 367-385.
29. K. Timachova, J. Newman and N. P. Balsara, *Journal of The Electrochemical Society*, 2019, **166**, A264.
30. A. Mistry, L. S. Grundy, D. M. Halat, J. Newman, N. P. Balsara and V. Srinivasan, *Journal of The Electrochemical Society*, 2022, **169**, 040524.
31. N. P. Balsara and J. Newman, *Journal of The Electrochemical Society*, 2022, **169**, 070535.
32. C. Sinistri, *The Journal of Physical Chemistry*, 1962, **66**, 1600-1601.
33. S. K. Ratkje, H. Rajabu and T. Førland, *Electrochimica Acta*, 1993, **38**, 415-423.
34. K. R. Harris, *Physical Chemistry Chemical Physics*, 2018, **20**, 30041-30045.
35. D. B. Shah, H. Q. Nguyen, L. S. Grundy, K. R. Olson, S. J. Mecham, J. M. DeSimone and N. P. Balsara, *Physical Chemistry Chemical Physics*, 2019, **21**, 7857-7866.
36. K. W. Gao, C. Fang, D. M. Halat, A. Mistry, J. Newman and N. P. Balsara, *ENERGY & ENVIRONMENTAL MATERIALS*, 2022, **5**, 366-369.
37. Y. Shao, H. Gudla, D. Brandell and C. Zhang, *Journal of the American Chemical Society*, 2022, **144**, 7583-7587.

38. M. Lorenz, F. Kilchert, P. Nürnberg, M. Schammer, A. Latz, B. Horstmann and M. Schönhoff, *The Journal of Physical Chemistry Letters*, 2022, **13**, 8761-8767.
39. F. Kilchert, M. Lorenz, M. Schammer, P. Nürnberg, M. Schönhoff, A. Latz and B. Horstmann, *arXiv preprint arXiv:2209.05769*, 2022.
40. Y. Choo, D. M. Halat, I. Villaluenga, K. Timachova and N. P. Balsara, *Progress in Polymer Science*, 2020, **103**, 101220.
41. A. Mistry, Z. Yu, B. L. Peters, C. Fang, R. Wang, L. A. Curtiss, N. P. Balsara, L. Cheng and V. Srinivasan, *ACS Central Science*, 2022, **8**, 880-890.
42. N. P. Balsara and J. Newman, *Electrochemical Systems, 4th Edition*, John Wiley & Sons, 2021.
43. H. G. Hertz, *Berichte der Bunsengesellschaft für physikalische Chemie*, 1977, **81**, 656-664.
44. L. A. Woolf and K. R. Harris, *Journal of the Chemical Society, Faraday Transactions 1: Physical Chemistry in Condensed Phases*, 1978, **74**, 933-947.
45. D. G. Miller, *The Journal of Physical Chemistry*, 1981, **85**, 1137-1146.
46. H. J. V. Tyrrell and K. R. Harris, *Diffusion in Liquids: A Theoretical and Experimental Study*, Butterworths, 1984.
47. H. J. Schoenert, *The Journal of Physical Chemistry*, 1984, **88**, 3359-3363.
48. N. P. Balsara and J. Newman, *Journal of The Electrochemical Society*, 2015, **162**, A2720-A2722.
49. I. Villaluenga, D. M. Pesko, K. Timachova, Z. Feng, J. Newman, V. Srinivasan and N. P. Balsara, *Journal of The Electrochemical Society*, 2018, **165**, A2766-A2773.
50. L. S. Grundy, D. B. Shah, H. Q. Nguyen, K. M. Diederichsen, H. Celik, J. M. DeSimone, B. D. McCloskey and N. P. Balsara, *Journal of The Electrochemical Society*, 2020, **167**, 120540.
51. D. Dong, F. Sälzer, B. Roling and D. Bedrov, *Physical Chemistry Chemical Physics*, 2018, **20**, 29174-29183.
52. S. Pfeifer, F. Ackermann, F. Sälzer, M. Schönhoff and B. Roling, *Physical Chemistry Chemical Physics*, 2021, **23**, 628-640.
53. B. R. Sundheim, *The Journal of Physical Chemistry*, 1956, **60**, 1381-1383.
54. A. Fernicola, F. Croce, B. Scrosati, T. Watanabe and H. Ohno, *Journal of Power Sources*, 2007, **174**, 342-348.
55. Y. Wang, K. Zaghib, A. Guerfi, F. F. C. Bazito, R. M. Torresi and J. R. Dahn, *Electrochimica Acta*, 2007, **52**, 6346-6352.
56. H. Sakaebe, H. Matsumoto and K. Tatsumi, *Electrochimica Acta*, 2007, **53**, 1048-1054.
57. H. Nakagawa, *Electrochemistry*, 2015, **83**, 707-710.
58. M. Gouverneur, F. Schmidt and M. Schönhoff, *Physical Chemistry Chemical Physics*, 2018, **20**, 7470-7478.
59. H. Sano, K. Kubota, Z. Siroma, S. Kuwabata and H. Matsumoto, *Journal of The Electrochemical Society*, 2019, **167**, 070502.
60. K. Kubota and H. Matsumoto, *ECS Transactions*, 2016, **75**, 585-590.
61. S. Lascaud, M. Perrier, A. Vallee, S. Besner, J. Prud'homme and M. Armand, *Macromolecules*, 1994, **27**, 7469-7477.
62. R. E. A. Dillon, C. L. Stern and D. F. Shriver, *Chemistry of Materials*, 2001, **13**, 2516-2522.
63. B. Roy, P. Cherepanov, C. Nguyen, C. Forsyth, U. Pal, T. C. Mendes, P. Howlett, M. Forsyth, D. MacFarlane and M. Kar, *Advanced Energy Materials*, 2021, **11**, 2101422.
64. H. Shobukawa, H. Tokuda, S.-I. Tabata and M. Watanabe, *Electrochimica Acta*, 2004, **50**, 305-309.
65. H. Shobukawa, H. Tokuda, M. A. B. H. Susan and M. Watanabe, *Electrochimica Acta*, 2005, **50**, 3872-3877.
66. R. Tao, D. Miyamoto, T. Aoki and T. Fujinami, *Journal of Power Sources*, 2004, **135**, 267-272.
67. R. Tao and T. Fujinami, *Journal of Power Sources*, 2005, **146**, 407-411.
68. G. Guzmán-González, M. Alvarez-Tirado, J. L. Olmedo-Martínez, M. L. Picchio, N. Casado, M. Forsyth and D. Mecerreyes, *Advanced Energy Materials*, **n/a**, 2202974.
69. O. Zech, M. Kellermeier, S. Thomaier, E. Maurer, R. Klein, C. Schreiner and W. Kunz, *Chemistry – A European Journal*, 2009, **15**, 1341-1345.
70. Y. Karatas, R. D. Banhatti, N. Kaskhedikar, M. Burjanadze, K. Funke and H.-D. Wiemhöfer, *The Journal of Physical Chemistry B*, 2009, **113**, 15473-15484.
71. P. G. Bruce, J. Evans and C. A. Vincent, *Solid State Ionics*, 1988, **28-30**, 918-922.
72. M. Watanabe, S. Nagano, K. Sanui and N. Ogata, *Solid State Ionics*, 1988, **28-30**, 911-917.
73. M. J. Frisch, G. W. Trucks, H. B. Schlegel, G. E. Scuseria, M. A. Robb, J. R. Cheeseman, G. Scalmani, V. Barone, G. A. Petersson, H. Nakatsuji, X. Li, M. Caricato, A. V. Marenich, J. Bloino, B. G. Janesko, R. Gomperts, B. Mennucci, H. P. Hratchian, J. V. Ortiz, A. F. Izmaylov, J. L. Sonnenberg, Williams, F. Ding, F. Lipparini, F. Egidi, J. Goings, B. Peng, A. Petrone, T. Henderson, D. Ranasinghe, V. G. Zakrzewski, J. Gao, N. Rega, G. Zheng, W. Liang, M. Hada, M. Ehara, K. Toyota, R. Fukuda, J. Hasegawa, M. Ishida, T. Nakajima, Y. Honda, O. Kitao, H. Nakai, T. Vreven, K. Throssell, J. A. Montgomery Jr., J. E. Peralta, F. Ogliaro, M. J. Bearpark, J. J. Heyd, E. N. Brothers, K. N. Kudin, V. N. Staroverov, T. A. Keith, R. Kobayashi, J. Normand, K. Raghavachari, A. P. Rendell, J. C. Burant, S. S. Iyengar, J. Tomasi, M. Cossi, J. M. Millam, M. Klene, C. Adamo, R. Cammi, J. W. Ochterski, R. L. Martin, K. Morokuma, O. Farkas, J. B. Foresman and D. J. Fox, *Journal*, 2016.
74. A. D. Becke, *The Journal of Chemical Physics*, 1993, **98**, 5648-5652.
75. C. Lee, W. Yang and R. G. Parr, *Physical Review B*, 1988, **37**, 785-789.
76. S. H. Vosko, L. Wilk and M. Nusair, *Canadian Journal of Physics*, 1980, **58**, 1200-1211.
77. P. J. Stephens, F. J. Devlin, C. F. Chabalowski and M. J. Frisch, *The Journal of Physical Chemistry*, 1994, **98**, 11623-11627.
78. B. J. Ransil, *The Journal of Chemical Physics*, 1961, **34**, 2109-2118.
79. S. F. Boys and F. Bernardi, *Molecular Physics*, 1970, **19**, 553-566.
80. M. D. Galluzzo, J. A. Maslyn, D. B. Shah and N. P. Balsara, *The Journal of Chemical Physics*, 2019, **151**, 020901.
81. K. Kubota and H. Matsumoto, *The Journal of Physical Chemistry C*, 2013, **117**, 18829-18836.
82. K. R. Harris and M. Kanakubo, *Journal of Chemical & Engineering Data*, 2016, **61**, 2399-2411.
83. H. K. Kashyap, H. V. R. Annapureddy, F. O. Raineri and C. J. Margulis, *The Journal of Physical Chemistry B*, 2011, **115**, 13212-13221.
84. T. Rüther, A. I. Bhatt, A. S. Best, K. R. Harris and A. F. Hollenkamp, *Batteries & Supercaps*, 2020, **3**, 793-827.

85. T. Koishi, S. Kawase and S. Tamaki, *The Journal of Chemical Physics*, 2002, **116**, 3018-3026.
86. T. Onak, H. Landesman, R. Williams and I. Shapiro, *The Journal of Physical Chemistry*, 1959, **63**, 1533-1535.
87. M. Moriya, D. Kato, W. Sakamoto and T. Yogo, *Chemical Communications*, 2011, **47**, 6311-6313.
88. S. Huang, X. Kong, Y. Xiong, X. Zhang, H. Chen, W. Jiang, Y. Niu, W. Xu and C. Ren, *European Polymer Journal*, 2020, **141**, 110094.
89. Y. Tanaka, J. Kaneko, M. Minoshima, Y. Iriyama and T. Fujinami, *Electrochemistry*, 2010, **78**, 397-399.